Cellular and Molecular Life Sciences (2026) 83:61
https://doi.org/10.1007/s00018-025-06042-8

ORIGINAL ARTICLE

Microbiome composition modulates the lethal outcome of Drosophila A virus infection

Rubén González[1] · Mauro Castelló-Sanjuán[1] · Ottavia Romoli[1] · Hervé Blanc[1] · Hiroko Kobayashi[2,3] · Jared Nigg[1,4] · Maria-Carla Saleh[1]

Received: 22 July 2025 / Revised: 12 December 2025 / Accepted: 13 December 2025

Abstract

Host-associated microbiomes can strongly influence viral infection outcomes, yet how minor variations in commensal bacterial composition modulate viral pathogenesis remain poorly understood. Here, we used *Drosophila melanogaster* to investigate how bacterial microbiome composition affects pathogenesis of enteric RNA viruses. *Lactiplantibacillus plantarum* supplementation increased bacterial microbiome diversity without altering total bacterial load, while *Acetobacter pomorum* supplementation had minimal impact on the bacterial microbiome. *L. plantarum*-enriched flies exhibited an additional ~ 15% reduction in lifespan from Drosophila A virus (DAV) infection despite showing reduced viral protein accumulation and similar viral RNA levels. The reduction in tolerance to viral infection required live bacteria and was observed only for DAV, as no change in mortality was observed with Nora virus or Drosophila C virus infections. Mechanistic investigations revealed that tolerance reduction occurs independently of transcriptional immune responses, as DAV-infected flies showed similar transcriptional profiles regardless of bacterial microbiome composition. Intestinal barrier function assays demonstrated that a large number of *L. plantarum*-supplemented flies died before developing signs of gut barrier disruption, suggesting that extra-intestinal mechanisms contribute to mortality; this interpretation is further supported by similar levels of intestinal damage markers observed in virus-infected flies under both microbiome conditions. Viral genomic sequencing ruled out microbiome-driven selection of more pathogenic viral variants, as no adaptive mutations were observed between microbiome conditions that could account for the differential pathogenesis. These findings describe how subtle shifts in microbiome composition modulate viral infection outcomes through pathways that operate independently of canonical immune responses, viral evolution, and intestinal damage.

Keywords Microbiome · Viral infections · *Drosophila melanogaster* · Disease tolerance · *Lactiplantibacillus plantarum* · Host-virus interactions

Introduction

Microbiomes shape host responses to viral infections across diverse biological systems [13, 14, 19, 21, 30, 35]. However, dissecting the tripartite interactions between virus, host, and microbiome remains challenging due to microbiome complexity and limited experimental tractability.

Drosophila melanogaster provides an ideal system for such investigations. It is a simple, manipulatable model system that offers powerful mechanistic approaches to understand these tripartite interactions. The fly gut microbiome is remarkably simple, typically containing only 1–30 bacterial taxa [4, 43], in contrast to the complex diversity associated with vertebrates (> 500 taxa) [4]. However, the composition of fly bacterial microbiomes is strongly influenced by

✉ Rubén González
ruben.gonzalez-miguelez@pasteur.fr

✉ Maria-Carla Saleh
carla.saleh@pasteur.fr

1 Institut Pasteur, Université Paris Cité, Viruses and RNA Interference Unit, Paris 75015, France

2 Division of Molecular Pathobiology, International Institute for Zoonosis Control, Hokkaido University, Sapporo, Hokkaido, Japan

3 Present address: Department of Molecular Virology, Research Institute for Microbial Diseases, The University of Osaka, Suita, Osaka, Japan

4 Present address: Biohub, San Francisco, CA, USA

Published online: 03 January 2026

host diet and laboratory conditions. Indeed, gut-associated bacteria of *Drosophila* stocks can differ greatly between laboratories [4, 7]. The most prevalent bacterial taxa in wild *Drosophila* are *Lactobacillales*, *Acetobacteraceae*, and *Enterobacteriaceae*, with most wild populations dominated by at least one of these [2, 7, 27]. Additionally, *Lactobacillus*, *Acetobacter*, and *Enterococcus* are commonly reported in laboratory-reared flies [4, 9, 33]. Within these dominant genera, natural populations commonly harbor multiple species: *Acetobacter* communities typically include *A. pomorum*, *A. tropicalis*, *A. orientalis*, and *A. persici*, while *Lactobacillus* communities are dominated by *L. plantarum* and *L. brevis*, with occasional presence of other species like *L. fructivorans* [7, 42, 47]. *A. pomorum* is one of the most prevalent acetic acid bacteria in wild-caught flies and laboratory populations [4, 8], and *Lactiplantibacillus plantarum* (formerly *Lactobacillus plantarum*, Zheng et al., [50] is consistently identified as a key member of laboratory reared *Drosophila* microbiome, alongside other *Lactobacillus* species [26, 27, 48]. Both *L. plantarum* and *A. pomorum* have been found in most laboratory stocks analyzed across multiple studies [4] and have well defined impacts on host physiology; *Acetobacter pomorum* modulates metabolic homeostasis through insulin signaling [39], while *Lactiplantibacillus plantarum* promotes growth under nutrient limitation by enhancing protein assimilation [37, 43]. Together, the compositional and functional simplicity of the fly gut microbiome, combined with the ecological relevance of these dominant species, enables its precise and biologically relevant manipulation.

To elucidate the interaction between virus, host, and microbiome, we focused on Drosophila A virus (DAV), a single-stranded positive-sense RNA virus that is present in both natural and laboratory populations [46]. DAV can be orally transmitted in laboratory settings, mimicking natural routes of infection [28]. DAV is an enteric virus that primarily infects the gut, which is the same niche occupied by commensal bacteria. Additionally, DAV infection disrupts intestinal homeostasis, reduces host lifespan, alters host locomotion, and accelerates host aging [6, 15, 29]. This infection phenotype presents a useful means to interpret how manipulating the host microbiome may impact the viral infection cycle and/or host responses to infection. Finally, DAV has a compact 5 kb genome encoding only two proteins: an RNA-dependent RNA polymerase (RdRp) and capsid protein (CP), making it a tractable subject for evolutionary analysis.

In this study, we systematically dissected the three-way interactions between DAV, the *Drosophila* host, and its bacterial microbiome. We demonstrate that bacterial strain composition impacts viral pathogenesis (here defined as the detrimental impact of the infection in the host lifespan) through mechanisms that operate independently of transcriptional immune responses, intestinal barrier dysfunction, and viral adaptive evolution. Our findings reveal that host-microbiome-virus interactions can modulate disease tolerance through previously uncharacterized pathways with consequences for viral pathogenesis.

Results

L. plantarum supplementation changes bacterial microbiome composition

We supplemented flies with bacteria to investigate how bacterial microbiome composition influences viral infection. We coated fly food with bacterial cultures starting one day before virus inoculation and continuing for five days post-inoculation, after which flies were maintained on standard food (Fig. 1A, methods). To prevent direct bacteria-virus interactions outside the host, we performed viral inoculations in non-supplemented tubes before transferring flies to bacteria-supplemented food.

We first characterized how supplementation affected the fly gut bacterial microbiome. When bacterial microbiomes from *A. pomorum* WJL (*Ap*)-supplemented flies were plated 12 days post supplementation, we found no evidence of the characteristic yellow colonies that distinguish this bacterial species, and overall bacterial load was significantly lower compared to controls, indicating that in our conditions *Ap* fails to colonize the gut (Fig. 1B). In contrast, *L. plantarum* WJL (*Lp*) supplementation substantially altered bacterial microbiome composition. *Lp* WJL cultures produce a variable number of morphologically distinct rough-edged colonies when plated at 30˚ C (Supplementary Fig. 1 A), a colony morphology absent in the bacterial microbiome of our laboratory w^{1118} fly stock. Following *Lp* supplementation, flies consistently harbored these characteristic rough-edged colonies that persisted well beyond the supplementation period and occurred independently of viral inoculation status (Supplementary Fig. 1B). Long-read sequencing of bacterial 16 S rDNA confirmed that only *L. plantarum* was detected in the flies, but different strains were detected in each condition: control flies (flies supplemented only with the broth media used to grow the bacterial cultures) harbored bacterial microbiomes dominated by two *L. plantarum* operational taxonomic units (OTUs), while *Lp*-supplemented flies contained more diverse *L. plantarum* OTU communities (Supplementary Fig. 2). Shannon diversity (H') analysis confirmed that *Lp* supplementation increased bacterial diversity (Fig. 1C, Supplementary File 1). *Lp* supplementation increased bacterial strain diversity without altering total bacterial load

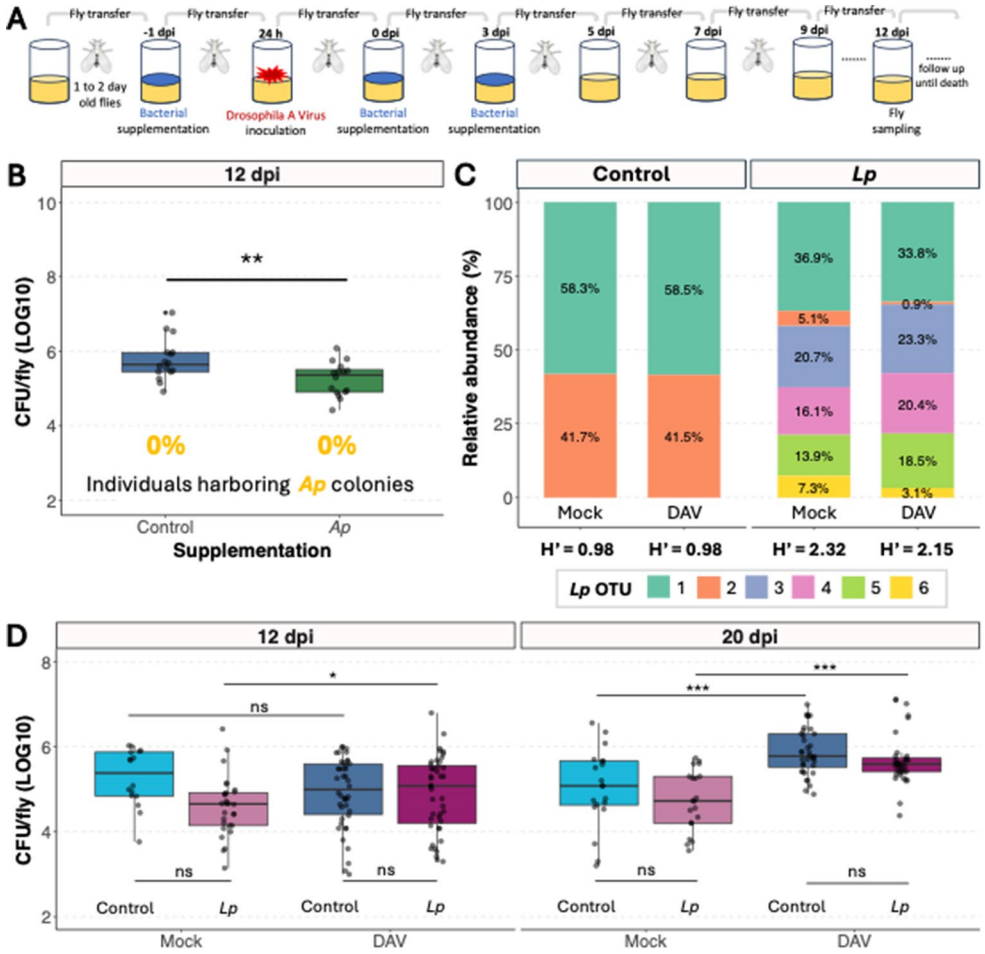

Fig. 1 Bacterial microbiome characterization following bacterial supplementation. (**A**) Experimental design schematic. (**B**) Colony-forming units (CFU) per individual at 12 dpi in DAV-inoculated flies that were *Ap*-supplemented or not. Statistical comparison performed using a t-test on $\log_{10}$-transformed data. (**C**) Metagenomic analysis showing the microbiota composition of control versus *Lp*-supplemented flies. Stacked bars show relative abundance of the six different *L. plantarum* operational taxonomic units (OTUs), with each color representing a different OTU. Shannon diversity indices (H') are displayed below each condition. Percentages within bars indicate relative abundance values. (**D**) Total bacterial load (CFU/fly, $\log_{10}$ scale) across treatment combinations at 12 and 20 dpi. Data show three experiments of Mock and DAV conditions for both control (non-supplemented) and *Lp* supplemented flies. Statistical analysis was performed using linear mixed-effects models with virus, treatment, and day as fixed factors and experiment as random factor, followed by pairwise comparisons using estimated marginal means with Tukey adjustment

(Fig. 1D), though viral infection increased bacterial loads in all groups at later timepoints.

Supplementation with live *Lp* reduces host tolerance to DAV infection

We orally inoculated flies with 1 OID_{50} of DAV, the dose that infects 50% of exposed individuals. Infection rates were consistent (~50%) across all treatments, indicating bacterial supplementation did not affect DAV infectivity (Fig. 2A). However, *Lp* supplementation produced contrasting effects on viral accumulation and pathogenesis. *Lp*-supplemented flies showed reduced viral protein levels at 12 days post-infection (dpi) compared to control flies (Fig. 2B), despite the viral RNA levels being similar at the same time point (Fig. 2C). Analysis of viral RNA kinetics during early infection (0, 2, and 7 dpi) revealed similar virus accumulation patterns between control and *Lp*-supplemented flies in both gut and carcass tissues, with viral RNA appearing first in the gut and spreading systemically by day 2 (Supplementary Fig. 3). This indicates that reduced protein levels were not due to altered viral dissemination or replication differences.

Reduced viral protein levels did not, however, correlate with decreased pathogenesis. DAV infection in non-supplemented controls reduced fly lifespan by ~20% compared to non-supplemented, mock-inoculated flies. DAV infection had a similar impact on lifespan in *Ap* supplemented flies compared to non-supplemented controls. In contrast, DAV-infected, *Lp*-supplemented flies showed ~35% lifespan reduction compared to mock-inoculated, *Lp*-supplemented

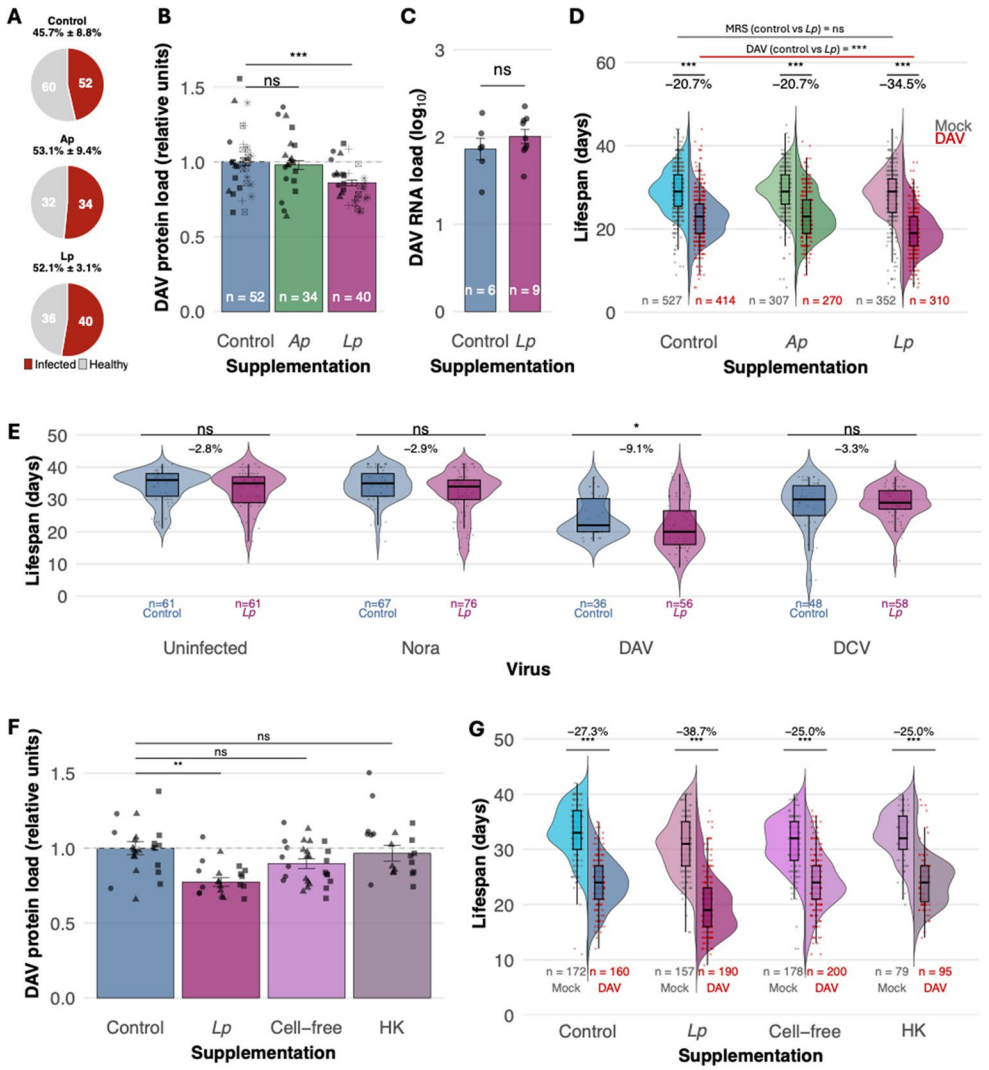

Fig. 2 Differential impact of bacterial microbiome composition on viral infection dynamics. (**A**) DAV infection prevalence in fly populations inoculated with 1 OID_{50} and supplemented with MRS (control), *A. pomorum* (*Ap*), or *L. plantarum* (*Lp*). (**B**) Viral capsid protein accumulation across treatment groups. Significance was calculated using a general linear-mixed model where the supplementation was the fixed factor and the experimental block a random effect. Different shapes represent independent experiments. (**C**) Comparative viral RNA accumulation in control versus *Lp*-supplemented flies. (**D**) Lifespan distribution showing DAV-induced lifespan reduction across bacterial treatment groups. Significance was calculated using a general linear-mixed model where the supplementation and infection status were the fixed factors and the experimental block a random effect. Six experiments were performed with several tubes per condition tested in each experiment. (**E**) Impact of *Lp*-enrichment on fly lifespan during infection with different persistent viruses. Significance was calculated using a general linear-mixed model where the supplementation was the fixed factor and the experimental block a random effect. (**F**) Viral capsid protein accumulation in flies supplemented with control, viable *Lp*, cell-free *Lp* supernatant, or heat-killed *Lp*. Significance was calculated using a general linear-mixed model where the supplementation was the fixed factor and the experimental block a random effect. Different shapes represent independent experiments. One experiment was performed with several tubes per condition tested. (**G**) Lifespan distribution of DAV-infected flies across *Lp* treatment conditions. Significance was calculated using a general linear-mixed model where the supplementation and infection status were the fixed factors and vial as a random effect. Two experiments were performed with several tubes per condition tested in each experiment

controls. This represents an additional ~ 15% reduction compared to DAV-infected, non-supplemented flies (95% CI: 13.6% to 17.4%, $P < 0.001$). This difference between bacterial microbiome conditions was statistically significant when comparing DAV-infected flies, while no significant differences were observed between mock-infected flies across treatments (Fig. 2D). Thus, *Lp* supplementation simultaneously reduced viral protein accumulation while enhancing virus-induced mortality.

To test whether the increased mortality observed after *Lp* supplementation was specific to a single-episode infections with DAV, we examined the effect of *Lp* supplementation in flies persistently infected with different RNA viruses. Similar to our observations with DAV single-episode infections,

Lp supplementation drove increased mortality in flies harboring persistent DAV infections compared to persistently infected non-supplemented flies (Fig. 2E). In contrast, flies persistently infected with Nora virus or Drosophila C virus (DCV) showed no survival changes under *Lp* supplementation, indicating that enhanced pathogenicity depends on DAV-specific interactions with the *Lp*-modified host environment.

We tested the bacterial requirements for modulating DAV pathogenesis using live *L. plantarum* cultures, cell-free supernatants, and heat-killed bacteria. Only viable bacteria reproduced both key phenotypes: reduced DAV protein accumulation (Fig. 2F) and enhanced mortality (Fig. 2G). Supernatants and heat-killed bacteria had no effect, demonstrating that viable bacteria are essential for modulating DAV pathogenesis.

Reduction of DAV tolerance occurs independently of transcriptional immune responses

To investigate potential mechanisms underlying bacterial microbiome-mediated reduction of DAV tolerance, we examined host transcriptional responses. Prior to viral inoculation, flies with different bacterial microbiome compositions showed minimal transcriptional differences, with changes limited to genes related to nutrition and metabolism (Supplementary Fig. 4).

We compared expression profiles of DAV-infected flies at 12 dpi to their respective mock-infected controls in both non-supplemented and *Lp*-supplemented flies. Both conditions mounted robust transcriptional responses to DAV infection, with hundreds of differentially expressed genes involved in immune defense, stress responses, and metabolic remodeling (Fig. 3A, B). In mock-inoculated conditions, *Lp* supplementation reduced the expression of only 4 genes compared to non-supplemented flies (Fig. 3C, Supplementary File 2): *pirk* (negative regulator of IMD immune signaling), *CG5550* (uncharacterized), *Pxn* (extracellular matrix protein with peroxidase activity involved in defense and phagocytosis), and *PKD* (serine/threonine kinase). These limited changes are consistent with known effects of *L. plantarum* on host development and metabolism [37, 43]. However, comparisons in DAV-infected flies revealed no significant differences between non-supplemented and *Lp*-supplemented flies (Fig. 3D). The absence of differentially expressed genes between bacterial microbiome conditions indicates that both non-supplemented and *Lp*-supplemented flies mount equivalent transcriptional responses to DAV infection.

Principal component analysis confirmed that infection status is the primary driver of transcriptional variance (PC1, 47%), while PC2 (20.7% variance) shows no clear separation by bacterial microbiome composition, confirming that the bacterial microbiome has a minimal influence on the fly's transcriptional response (Fig. 3E).

Given that transcriptional analysis cannot capture all aspects of immune function and considering the critical role of *Sting*-mediated innate immunity in DAV pathogenesis [29], we tested whether this pathway mediates the bacterial microbiome-dependent reduction in viral tolerance. We supplemented *Sting* mutant flies with *Lp* and challenged them with DAV. *Lp*-supplemented *Sting* mutants exhibited approximately 10% additional reduction in lifespan compared to non-supplemented *Sting* mutants, similar to the effect observed in wild-type flies (Fig. 3F). This demonstrates that the bacterial microbiome's impact on host tolerance to DAV operates independently of Sting signaling, further supporting a mechanism that functions outside canonical antiviral immune pathways.

Reduced DAV tolerance operates independently of intestinal pathology

To assess whether microbiome-mediated enhancement of DAV pathogenesis involves altered intestinal barrier function, we employed the "Smurf" assay, which uses a non-toxic blue dye to visualize gut barrier permeability [34]. In mock-infected flies with control microbiomes, we observed the Smurf phenotype (indicating barrier disruption) in the days before death, establishing the normal progression of intestinal aging. As expected, DAV-infected flies with control microbiomes showed shorter lifespans and earlier appearance of Smurf phenotypes, with a reduced interval between barrier disruption and death (Fig. 4A,B). This suggests that once the intestinal barrier is compromised, systemic effects accelerate mortality beyond what would be expected from intestinal damage alone.

During DAV infection, *Lp*-supplemented flies exhibited the expected reduction in lifespan that we observed consistently across experiments. However, the median time to Smurf of *Lp*-supplemented and control-supplemented flies was similar during DAV infections (Fig. 4A,B). This indicates that many flies died before showing signs of intestinal barrier disruption, suggesting that *Lp* supplementation reduces the host tolerance to DAV through mechanisms acting beyond the gut.

To further investigate intestinal effects, we quantified phospho-histone H3 (PH3)-positive cells in the midgut, a marker of intestinal stem cell (ISC) proliferation and epithelial damage response [29]. While DAV infection significantly increased the number of PH3-positive cells compared to mock infection, *Lp* supplementation did not further alter this proliferative response at 12 dpi (Fig. 4C). This finding supports the observation that enhanced pathogenesis in

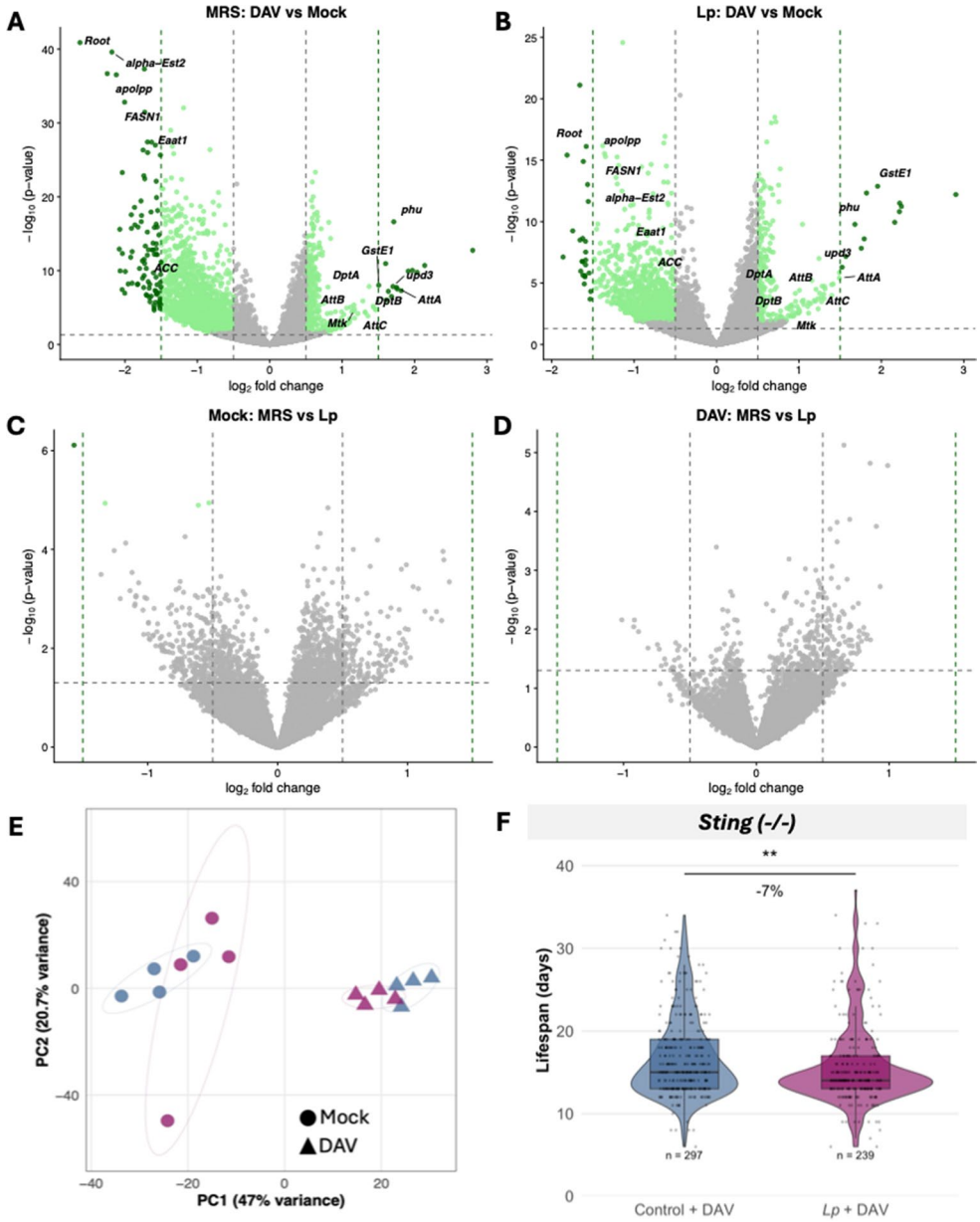

Fig. 3 Transcriptional responses in each bacterial microbiome. **A-B)** Volcano plots showing differential gene expression in response to DAV infection (DAV-infected vs. mock-infected flies) in non-supplemented (MRS) flies (**A**) and *Lp*-supplemented flies (**B**) at 12 dpi. The x-axis represents $\log_2$ fold change and the y-axis represents $-\log_{10}$ adjusted p-value. Horizontal dashed line indicates significance threshold (adjusted $P<0.05$) and vertical dashed lines indicate fold change thresholds ($|\log_2 FC| = 0.5$). Green dots represent significantly differentially expressed genes, with darker green indicating higher magnitude changes ($|\log_2 FC| > 1.5$). Gray dots represent genes that do not meet significance criteria. Selected genes are labeled. Both bacterial microbiome conditions show similar transcriptional responses to DAV infection, with comparable numbers of differentially expressed genes and similar expression patterns. **C-D)** Direct comparison of gene expression between bacterial microbiome conditions. Volcano plots comparing *Lp*-supplemented versus non-supplemented flies in DAV-infected (**C**) and mock-infected (**D**) conditions. Horizontal dashed line indicates significance threshold (adjusted $P<0.05$) and vertical dashed lines indicate fold change thresholds ($|\log_2 FC| = 0.5$). No genes show significant differential expression between bacterial microbiome conditions in either infected or uninfected flies, demonstrating that the reduced tolerance observed in *Lp*-supplemented flies occurs independently of transcriptional changes. **E)** Principal component analysis (PCA) of genome-wide gene expression profiles using variance-stabilized transformed counts. Each point represents a biological replicate (pool of 5 flies). Circles represent mock-infected samples and triangles represent DAV-infected samples. Blue indicates non-supplemented (MRS) conditions and purple/pink indicates *Lp*-supplemented conditions. **F)** Lifespan analysis of *Sting* mutant flies infected with DAV under different bacterial microbiome conditions. Violin plots show the distribution of individual fly lifespans, with horizontal lines indicating median values and quartiles. Each dot represents the lifespan of an individual fly. Statistical comparison performed using linear mixed-effects models with bacterial supplementation as fixed factor and vial as a random effect. Sample sizes are indicated on the plot. Each sample in panels A-D represents a pool of 5 flies ($n=4$ biological replicates per condition)

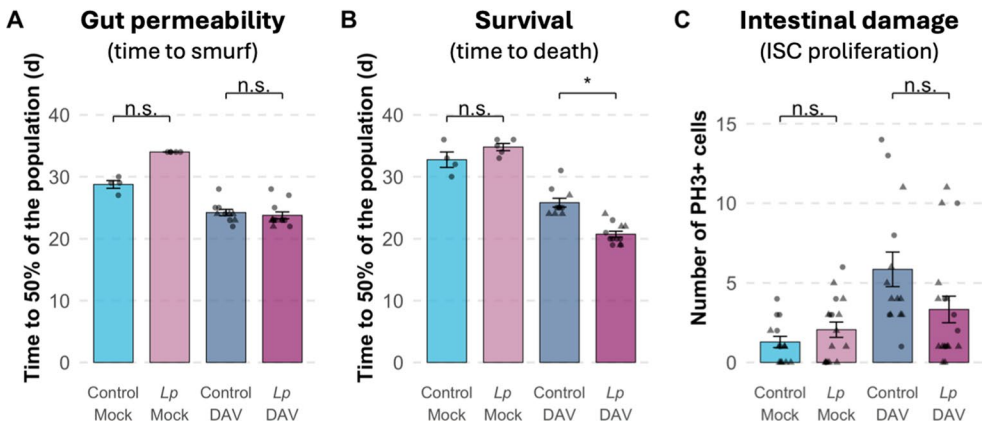

Fig. 4 Reduced tolerance in *Lp*-supplemented flies operates through extra-intestinal mechanisms. **A-B**) Gut barrier permeability and survival measured in the same cohorts of flies. (**A**) Bars show the median time for 50% of the population to exhibit the Smurf phenotype (intestinal barrier disruption). DAV infection accelerates barrier disruption in both bacterial microbiome conditions. *Lp* supplementation does not significantly alter the timing of barrier disruption in either mock or DAV-infected flies. (**B**) Fly survival in the same experimental cohorts. DAV infection reduces lifespan in both conditions, with *Lp*-supplemented flies showing significantly greater lifespan reduction. **C**) Intestinal stem cell (ISC) proliferation quantified by PH3-positive cells in the midgut at 12 dpi. DAV infection significantly increases ISC proliferation compared to mock infection in both bacterial microbiome conditions, but *Lp* supplementation does not further enhance this proliferative response. This indicates that reduced tolerance in *Lp*-supplemented flies does not result from enhanced local intestinal damage. Data are presented as mean ± SE with individual data points shown. Statistical comparisons were performed using linear mixed-effects models with bacterial supplementation and infection status as fixed factors and vial as random effect. n.s., not significant; $*P < 0.05$

Lp-supplemented flies does not result from increased local intestinal damage.

Increased host mortality is not caused by the emergence of new viral variants

Given the observed differences in capsid protein accumulation and DAV pathogenesis between *Lp*-supplemented and non-supplemented bacterial microbiomes, we tested whether certain bacterial communities selected for more pathogenic viral variants during infection. To test this, we sequenced DAV genomes from flies with non-supplemented and *Lp*-supplemented bacterial microbiomes after 12 days of infection.

We identified 128 mutations across the viral genome, revealing three distinct evolutionary patterns: 45 mutations shared between conditions, 38 non-supplemented-specific, and 45 *Lp*-specific mutations (Supplementary Fig. 5). Even within only 12 days, mutations with a notable frequency change (≥20%) were common in both conditions. Mutations were predominantly transitions over transversions and were distributed throughout the RdRp and capsid genes. Non-supplemented-specific mutations showed greater mean frequency increases (17.9 ± 3.8%) than *Lp*-specific ones (11.6 ± 1.1%), with a similar pattern in shared mutations (12.1 ± 3.2% increase in non-supplemented vs. 6.7 ± 1.9% in *Lp*). Over half of all mutations were novel, meaning they arose during the 12-day infection rather than being minor variants already present in the virus population used as inoculum. Despite this quasispecies diversity, no mutations reached fixation in any of the four biological replicates, and no fixed mutations were identified that could account for the differential pathogenesis observed between microbiome conditions. These results demonstrate that while bacterial microbiome composition can influence viral population dynamics, the increased mortality in *Lp*-supplemented flies is not driven by selection of more pathogenic viral variants.

Discussion

Our study demonstrates that subtle bacterial microbiome alterations can reshape virus-host interactions through pathogen-specific mechanisms that operate independently of canonical immune transcription and viral evolution. *Lp* supplementation selectively enhanced DAV pathogenesis while not affecting survival during Nora virus or DCV infections, revealing the specificity of microbiome-virus interactions. This selectivity likely reflects diverse viral strategies in tropism, replication, and host response activation [6, 22, 36, 38, 40]. Similar virus-specific interactions occur in other systems: human norovirus requires specific bacteria for cell infection [18], while influenza pathogenesis varies with the bacterial species present [17]. Our findings align with recent work [44] examining microbiome reconstitution across four *Drosophilidae* species challenged *via* septic injury with bacterial pathogens or DCV. They found highly species-specific and pathogen-specific effects, with the magnitude and direction depending on the host-pathogen combination. We similarly observed pathogen-specific

effects with viral oral infection, where *L. plantarum* supplementation reduced tolerance to DAV but not to Nora virus or DCV, despite the shared gut compartment potentially favoring stronger microbiome-pathogen interactions.

The paradoxical reduction in viral protein levels alongside enhanced mortality indicates a decoupling of viral burden from pathogenesis, a pattern that distinguishes tolerance from resistance mechanisms. Resistance reduces pathogen load through immune-mediated elimination, while tolerance limits tissue damage and maintains physiological function despite infection [32, 41]. Our finding that *L. plantarum* supplementation reduces host tolerance (ability to limit damage for a given pathogen load) rather than resistance (ability to limit pathogen burden) suggests that the microbiome modulates host responses to infection-induced damage rather than controlling viral replication directly. This distinction is critical because tolerance mechanisms can determine disease outcomes independently of pathogen burden and represent potential therapeutic targets that do not drive pathogen evolution [23]. The observation that flies with lower viral protein levels nonetheless exhibited greater mortality exemplifies impaired tolerance: these flies were less capable of withstanding the physiological stress imposed by viral infection despite reduced viral burden.

Commensal bacteria influencing host-pathogen interactions is well-documented across diverse organisms [1, 3, 5, 16]. However, our findings in *Drosophila* identify a tolerance-reduction mechanism that operates through non-canonical pathways. Three independent lines of evidence support this conclusion. First, transcriptional profiling revealed no gene expression differences between microbiome conditions, ruling out immune transcriptional responses. Second, intestinal pathology markers were similar across conditions, excluding gut damage as the driver. Third, the effect persisted in Sting-deficient flies, showing independence a pathway critical for DAV pathogenesis.

Several non-mutually exclusive mechanisms warrant investigation. First, live *L. plantarum* may continuously produce metabolites that alter host cellular processes in ways that exacerbate viral pathology without changing steady-state gene expression. The requirement for viable bacteria (as heat-killed bacteria and supernatants had no effect) indicates that ongoing bacterial metabolism is essential. Second, bacterial enzymatic activities could modify host glycoproteins, lipids, or other biomolecules in ways that affect viral dissemination, cellular damage, or tissue-specific susceptibility. This possibility is exemplified by the *Serratia marcescens* protein that digests mucins in mosquito gut to enhance arboviral transmission [49]. Third, post-transcriptional regulation could explain how microbiome composition affects pathogenesis without transcriptional signatures. Finally, the microbiome may alter host metabolic states that specifically affect cellular responses to DAV infection in ways that manifest only under the stress of viral replication.

Our viral genomic analysis revealed substantial mutational diversity arising within 12 days but no evidence that different microbiome conditions selected for more pathogenic viral variants. This supports that enhanced mortality results from altered host tolerance rather than viral adaptation to bacterial environments. The 12-day infection period may be sufficient to generate viral diversity but too short for mutations to reach frequencies that could drive the observed pathological differences. Our finding contrasts with longer-term infections in other systems where microbiome composition can drive pathogen evolution [12, 20]. We nevertheless acknowledge that according to quasispecies theory, low-frequency viral variants can influence pathogenesis even without reaching fixation, and minor variants have been shown to affect virulence in RNA virus populations [11, 24, 45].

Several limitations should be taken into consideration when interpreting our results. First, while we have identified a reproducible and biologically significant phenotype, the underlying mechanism remains unresolved. Our data effectively rule out transcriptional immune responses and viral evolution as primary drivers, but the actual molecular and cellular mechanisms require further investigation. Second, we focused on bacterial components of the microbiome; fungal and archaeal community members may also contribute to the observed effects. Third, our study examined only female flies at a single temperature (29 °C); sex-specific differences and temperature-dependent effects may exist. Fourth, we examined a limited number of viruses; the generalizability of these findings across different viral families remains to be determined.

Our results establish a novel phenotype in microbiome-virus interactions and provide a foundation for future mechanistic investigations. The finding that bacterial microbiome composition can significantly alter host tolerance to viral infection independently of immune transcriptional responses, viral evolution, and intestinal pathology opens new avenues for understanding how commensal bacteria influence disease outcomes.

Materials and methods

Animal strains and maintenance

We used mated female w^{1118} flies for all experiments unless otherwise specified. The *Sting* mutant line contains the dSting^{Rxn} mutation and was a gift from J.L. Imler (Université de Strasbourg, France). We maintained all fly stocks on a cornmeal diet; each tube had approximately 7 mL of fly food,

that was prepared by combining 440 g inactive dry yeast, 440 g corn meal, and 60 g agar in 6 L osmotic water. The mixture was autoclaved and after cooling, 150 ml moldex solution (20% methylhydroxybenzoate) and 29 ml propionic acid were added as preservatives. Flies were kept at 25 °C under a 12:12 h light: dark cycle and transfer to 29 °C upon eclosion to perform the experiments. All stocks were verified to be free of *Wolbachia* infection.

Bacterial culture

Flies were supplemented with bacteria by coating the fly food surface with 10^8 CFU of a bacterial culture or MRS as a control (non-supplemented). We cultured *A. pomorum* strain WJL in 10 ml of MRS broth in 20 ml flasks at 30 °C with 180 rpm agitation for 20 h. We grew *L. plantarum* strain WJL in 10 ml of MRS broth (Carl Roth, Germany) in 15 ml culture tubes at 37 °C without agitation for 20 h. For CFU quantification, we plated serial dilutions on MRS agar and incubated plates for 48 h at 30 °C or 24 h at 37 °C.

To prepare cell-free supernatant, we pelleted 2 ml of a 10^9 CFU/ml bacterial culture by centrifugation at 5000 rpm for 10 min and filtered the supernatant through a 0.22 µm filter. For heat-killed cultures, we incubated 1 ml of 10^9 CFU/ml culture at 100 °C for 10 min. We verified the absence of viable cells in both preparations by plating 50 µl on MRS agar and confirming no colony growth after 48 h of incubation at 30 °C.

Viruses

We orally inoculated mated female flies 1–2 days post-eclosion. After maintaining males and females together at 29 °C for 24 h, we removed males and transferred females to empty vials for three hours of starvation. We then moved flies to vials containing food coated with 100 µl of DAV stock (1–2 OID_{50}) and maintained groups of 20–30 flies per vial for 24 h. We designated the transfer time to fresh vials as 0 dpi and transferred flies to new vials every 2–3 days thereafter. Mock inoculations followed the same procedure using filtered extract from uninfected flies.

For persistent infections, we used persistently infected flies from Nigg and colleagues [29]. The stocks were maintained at 25 °C under a 12:12 light: dark cycle.

Preparation of viral inoculum

We prepared DAV stocks from persistently infected w^{1118} flies following Nigg et al. [29]. We homogenized 60 mixed-age flies in 300 µl PBS, snap-froze the homogenate, and clarified it by two rounds of centrifugation (15,000 × g, 10 min, 4 °C). After filtering through a 0.22 µm filter, we prepared 100 µl aliquots for storage at −80 °C. We prepared mock stock identically using uninfected flies.

We determined viral titer via 50% endpoint dilution [28], using ELISA to assess infection status at 12 dpi in flies exposed to serial dilutions of viral stock. For experiments, we used 1:5 dilutions from the stock for the 1000 OID inoculum and 1:500 for the 1 OID inoculum.

Enzyme-linked immunosorbent assay (ELISA)

We detected DAV infection by ELISA following Nigg et al. [28]. We homogenized individual flies in 100 µl PBS and mixed 20 µl homogenate with 20 µl lysis buffer (40 mM HEPES pH 7.5, 2 mM DTT, 200 µM KCl, 10% glycerol, 0.1% NP-40, 1× complete EDTA-free Protease Inhibitor Cocktail (Roche, 11873580001). After 15 min at room temperature, we added 10 µl of this mixture to 190 µl of 0.05 M carbonate-bicarbonate buffer (pH 9.6) in MaxiSorp plates (Thermo Fisher, 442404) and incubated for 2 h at room temperature.

We washed plates three times with PBS-T (1× PBS, 0.05% Tween-20), blocked with PBS-T containing 5% non-fat dry milk (2 h at room temperature), and incubated overnight at 4 °C with a polyclonal anti-DAV CP antibody (1:2000). After washing, we added donkey anti-rabbit IgG-HRP (Cytiva, NA934; 1:2000) for 2 h at room temperature, washed, and developed with TMB substrate (Thermo Fisher, 34022). We stopped the reaction with 2 N HCl and measured absorbance at 450 nm in a plate reader (Tecan Infinite M200 PRO). We defined infection as A_{450} values exceeding the mock average plus three standard deviations.

For viral protein quantification, we used the absorbance values at 450 nm as a measure of viral capsid protein abundance. We normalized all values within each plate by dividing by the mean absorbance of DAV-positive non-supplemented samples on that plate. The normalized values are presented as viral capsid protein accumulation.

Lifespan analysis

We conducted lifespan experiments using three to six biological replicates with 20–25 female flies per replicate, sorted at five days post-infection. We maintained flies at 29 °C under the specific vial conditions described for each experiment. We monitored survival daily by counting dead flies in each vial and transferred flies to fresh vials every three to four days.

Smurf assay

We assessed intestinal barrier function using the Smurf assay with biological replicates of 20 female w^{1118} flies, set

up as described for survival analysis. Beginning at 7 dpi, we continuously maintained flies in vials containing food supplemented with 100 µl of sterile 16% FD&C blue dye. We scored "Smurfness" (blue dye leakage throughout the body) daily by examining flies according to Martins et al. [25].

RNA extraction

We extracted total RNA from whole flies by resuspending 100 µl of fly homogenate (in PBS buffer) in 400 µl TRIzol Reagent (Invitrogen, 15596026), vortexed thoroughly, and incubated for 3 min at room temperature. We added 100 µl chloroform, vortexed again, and incubated for another 3 min before centrifuging at 12,000 × g for 15 min at 4 °C. We collected the upper aqueous phase and added an equal volume of 100% isopropanol and 1 µl of GlycoBlue (ThermoFisher Scientific), vortexed thoroughly, and incubated for 3 min at room temperature. We then centrifuged at 12,000 × g for 10 min at 4 °C. After discarding the supernatant, we washed the RNA pellet with 500 µl of 75% ethanol, inverted 10 times to mix, and centrifuged at 7,500 × g for 5 min at 4 °C. We removed the supernatant, air-dried the tube, dissolved the RNA pellet in 20 µl Milli-Q water, and incubated at 55 °C for 10 min. We measured RNA concentration using the Qubit RNA BR Assay Kit (Invitrogen, Q10211).

Immunofluorescence of digestive tissues

We dissected whole digestive tracts in 1× PBS over a 20-minute period and immediately fixed them in 4% paraformaldehyde for an additional 50 min. We washed fixed tissues three times (10 min each) in 1× PBS with 0.1% Triton X-100 (PBT), incubated them in 1× PBS with 50% glycerol for 30 min, and equilibrated them in 1× PBT for 30 min. We then incubated tissues with anti-PH3 primary antibody (rabbit, 1:1000, Merck Millipore, 06–570) diluted in 1× PBT overnight at 4 °C. After three 10-minute washes, we incubated tissues with anti-rabbit Alexa Fluor 647 secondary antibody for 3–5 h at room temperature. We performed three final 10-minute washes, with the last wash containing 1 µg/ml DAPI, and mounted tissues in 4% N-propyl-gallate in 80% glycerol. We imaged samples using a Zeiss LSM 700 confocal microscope at the Institut Pasteur Photonic BioImaging facility and manually counted PH3-positive cells throughout the entire midgut.

Quantitative reverse transcription polymerase chain reaction (RT-qPCR)

We performed reverse transcription on total RNA using random primers and Maxima H Minus Reverse Transcriptase (Thermo Scientific, EP0751) according to the manufacturer's instructions. We diluted the resulting cDNA 1:10 with nuclease-free water and performed qPCR in triplicate 10 µl reactions using virus-specific primers (Supplementary Table 1). The thermal cycling protocol consisted of 2 min at 50 °C, 10 min at 95 °C, followed by 40 cycles of 15 s at 95 °C and 60 s at 60 °C, with a standard melt curve analysis after amplification. We set the threshold for viral RNA detection at Ct 35, considering samples with higher Ct values as uninfected. We normalized virus Ct values against the *Rp49* housekeeping gene and presented results as log10 of $2^{-\Delta Ct}$ values.

High-throughput sequencing

We performed RNA sequencing on 4 biological replicates per experimental condition. We collected flies at 12 dpi from four treatment groups (control + mock, control + DAV, *Lp* + mock, *Lp* + DAV) and also sequenced samples from both supplementation conditions immediately before virus inoculation. We confirmed infection status by ELISA and prepared 4 pools of 5 individuals per condition. We prepared RNA-seq libraries from 15 ng of pooled RNA (3 ng per individual) using the NEBNext Ultra II RNA Library Prep Kit (New England Biolabs, E7770L) with NEBNext Multiplex Oligos (Dual Index Primers Set 1; New England Biolabs, E7600S). We performed all sequencing on an Illumina NextSeq 500 instrument using a NextSeq 500/550 High Output Kit v2.5 (75 cycles; Illumina, 20024906).

Bacterial microbiome composition sequencing

We collected 60 female flies per condition at 12 dpi. We surface-sterilized flies to remove external microbes through sequential washes: 10% bleach for 5 min, 70% ethanol for 5 min, followed by three rinses in sterile water. We added lysis buffer (10 mM Tris-HCl pH 8, 26 mM EDTA, 0.5% SDS, 5 mg/ml lysozyme) to the flies and then homogenized with sterile pestles. After incubating lysates for 1 h at 37 °C, we extracted total DNA using the DNeasy Blood and Tissue Kit (Qiagen) following the manufacturer's protocol.

We amplified the 16 S rRNA gene using 100 ng genomic DNA as template in 50 µl final reaction volume. We employed 27 F and 1391R primers (Supplementary Table 1) and performed PCR using Phusion High Fidelity Polymerase (Thermo Fisher), using 1 U of enzyme and a final primer concentration of 400 nM. The PCR cycle was: an initial denaturation step of 5 min at 98 ˚ C followed by 35 cycles of 98 ˚ C for 15 s, 60 ˚ C for 20 s and 72 ˚ C for 1 min, followed by a final extension at 72 ˚ C for 10 min. PCR amplicons were purified using the NucleoSpin gel and PCR clean-up purification kit (Macherey Nagel) and sequenced by Plasmidsaurus using Nanopore. Between 28,522 and 51,439 reads were obtained per sample.

We quality-checked the resulting long-reads using NanoPlot (version 1.42.0) and filtered them with filtlong (version 0.2.1), discarding reads with average quality scores below Q17 and read lengths outside the 1200–1500 bp range. Reads were then denoised and chimeras were removed using dada2 in qiime2 (version 2019.10). OTU taxonomy was assigned using the Silva database.

Genome analysis

We trimmed 15 nucleotides from the 5′ end of raw sequencing reads and removed reads with quality scores below 30. We mapped the clean reads to the *D. melanogaster* genome (release dmel-r6.56) using STAR version 2.7.11b [10]. We performed feature counting with HTSeq version 0.11.2 [31] and differential gene expression analysis with DESeq2 in R Studio (version 2023.03.1). We filtered genes with fewer than 10 total counts across all samples and applied log2 fold change shrinkage using the "normal" method. We identified differentially expressed genes between DAV-infected and mock-inoculated flies within each bacterial microbiome condition and performed variance stabilizing transformation for visualization. We considered only adjusted p-values for statistical significance.

For viral genomic analysis, we first sequenced our DAV inoculum and mapped it to a reference DAV genome (GenBank accession no. FJ150422.1) to establish a stock-specific reference sequence. We processed experimental samples by filtering reads shorter than 40 nucleotides using cutadapt and trimmed 17 nucleotides from the 5' end of reads. We aligned the processed reads to the reference genome using HiSAT2 version 2.2.1 with parameters optimized for viral sequences (--no-spliced-alignment, --score-min L,0.0,−0.8). We converted alignments to sorted BAM format using samtools and assessed viral load using samtools *flagstat*. For variant detection, we applied indel quality correction using LoFreq *indelqual*, followed by variant calling with LoFreq using a minimum coverage threshold of 5 reads and significance level of 0.05.

Statistical analysis

We performed all statistical analyses in R version 4.3.2 using the Rstudio development environment version 2023.12.1+402. Statistical significance was defined as adjusted $P<0.05$, with symbols representing significance levels as follows: *** $P<0.001$; ** $P<0.01$; * $0.01<P<0.05$.

We applied generalized linear models (GLM) using the glm function from the "stats" package and linear mixed-effects models (LMM) using the lmer function from the "lme4" package version 1.1–35.5, selecting the appropriate model based on data structure and experimental design. For post-hoc analyses, we conducted pairwise comparisons using the *emmeans* function from the "emmeans" package version 1.10.5, applying Tukey's correction to control for multiple testing. Detailed descriptions of the specific statistical approaches used for each analysis are provided in the corresponding figure legends.

Supplementary information The online version contains supplementary material available at https://doi.org/10.1007/s00018-025-06042-8.

Acknowledgements We thank François Leulier laboratory for sharing the bacterial strains. We thank members of the Saleh lab for fruitful discussion, Cassandra Koh for assistance with experiments, and Anamarija Butković for guidance in the phylogenetic analysis. We are grateful to Christophe Neuens, Harouna Tandjigora, and Alexis Matamoro-Vidal from Institut Pasteur for their dedicated work in preparing fly food media and ensuring consistent, high-quality rearing conditions for our experiments.

Author contributions **Rubén González**: conceptualization, data curation, formal analysis, investigation, visualization, writing-original draft, writing-review, supervision, and editing. **Mauro Castelló-Sanjuán**: investigation. **Ottavia Romoli**: investigation, formal analysis, writing-review, and editing. **Hervé Blanc**: investigation. **Hiroko Kobayashi**: investigation. **Jared Nigg**: writing-review, supervision. **Maria-Carla Saleh**: conceptualization, funding acquisition, project administration, resources, supervision, writing-review, and editing. All authors gave final approval for publication.

Funding Rubén González is supported by a Pasteur-Roux-Cantarini fellowship of Institut Pasteur. This work was supported by funding from the French Government's Investissement d'Avenir program, Laboratoire d'Excellence Integrative Biology of Emerging Infectious Diseases (grant ANR-10-LABX-62-IBEID), the Agence Nationale de la Recherche (grant ANR-23-CE15-0038-01, INFINITESIMAL), the Fondation iXcore - iXlife - iXblue Pour La Recherche and the Explore Donation, MIE project to Maria-Carla Saleh. This project has received funding from the European Union's Horizon 2020 research and innovation program under the Marie Skłodowska-Curie grant agreement No 101024099 to Jared Nigg.

Data availability Raw sequencing reads can be found in the Sequence Read Archive under the BioProject PRJNA1293387. All other data supporting the findings are available within the article and supplementary files.

Declarations

Competing interests The authors have no relevant financial or non-financial interests to disclose.

References

1 Abt MC, Osborne LC, Monticelli LA et al (2012) Commensal bacteria calibrate the activation threshold of innate antiviral immunity. Immunity 37:158–170. https://doi.org/10.1016/j.immuni.2012.04.011

2 Adair KL, Wilson M, Bost A, Douglas AE (2018) Microbial community assembly in wild populations of the fruit fly drosophila melanogaster. ISME J 12:959–972. https://doi.org/10.1038/s41396-017-0020-x

3 Belkaid Y, Harrison OJ (2017) Homeostatic immunity and the microbiota. Immunity 46:562–576. https://doi.org/10.1016/j.immuni.2017.04.008

4 Broderick NA, Lemaitre B (2012) Gut-associated microbes of *Drosophila melanogaster*. Gut Microbes 3:307–321. https://doi.org/10.4161/gmic.19896

5 Broderick NA, Buchon N, Lemaitre B (2014) Microbiota-induced changes in <Emphasis Type="Italic">Drosophila melanogaster</Emphasis> host gene expression and gut morphology. mBio. https://doi.org/10.1128/mbio.01117-14

6 Castelló-Sanjuán M, González R, Romoli O, Blanc H, Nigg J, Saleh MC (2025) Persistent viral infections impact key biological traits in *Drosophila melanogaster*. PLoS Biol 23:e3003437. https://doi.org/10.1371/journal.pbio.3003437

7 Chandler JA, Morgan Lang J, Bhatnagar S et al (2011) Bacterial communities of diverse drosophila species: ecological context of a host–microbe model system. PLoS Genet 7:e1002272. https://doi.org/10.1371/journal.pgen.1002272

8 Corby-Harris V, Pontaroli AC, Shimkets LJ et al (2007) Geographical distribution and diversity of bacteria associated with natural populations of Drosophila melanogaster. Appl Environ Microbiol 73:3470–3479. https://doi.org/10.1128/aem.02120-06

9 Cox CR, Gilmore MS (2007) Native microbial colonization of *Drosophila melanogaster* and its use as a model of *Enterococcus faecalis* pathogenesis. Infect Immun 75:1565–1576. https://doi.org/10.1128/iai.01496-06

10 Dobin A, Davis CA, Schlesinger F et al (2013) STAR: ultrafast universal RNA-seq aligner. Bioinformatics 29:15–21. https://doi.org/10.1093/bioinformatics/bts635

11 Domingo E, Sheldon J, Perales C (2012) Viral quasispecies evolution. Microbiol Mol Biol Rev 76:159–216. https://doi.org/10.1128/MMBR.05023-11

12 Ford SA, Kao D, Williams D, King KC (2016) Microbe-mediated host defence drives the evolution of reduced pathogen virulence. Nat Commun 7:13430. https://doi.org/10.1038/ncomms13430

13 Fraune S, Bosch TC (2010) Why bacteria matter in animal development and evolution. BioEssays 32:571–580. https://doi.org/10.1002/bies.200900192

14. González R, Elena SF (2021) The interplay between the host microbiome and pathogenic viral infections. mBio 12:e02496–e02421. https://doi.org/10.1128/mBio.02496-21

15. González R, Castelló-Sanjuán M, Saleh MC (2025) Viral infections reduce Drosophila lifespan through accelerated aging. bioRxiv 3(13):643076 https://doi.org/10.1101/2025.03.13.643076

16 Hooper LV, Littman DR, Macpherson AJ (2012) Interactions between the microbiota and the immune system. Science 336:1268–1273. https://doi.org/10.1126/science.1223490

17 Ichinohe T, Pang IK, Kumamoto Y et al (2011) Microbiota regulates immune defense against respiratory tract influenza A virus infection. Proc Natl Acad Sci USA 108:5354–5359. https://doi.org/10.1073/pnas.1019378108

18 Jones MK, Watanabe M, Zhu S et al (2014) Enteric bacteria promote human and mouse Norovirus infection of B cells. Science 346:755–759. https://doi.org/10.1126/science.1257147

19 Karst SM (2016) The influence of commensal bacteria on infection with enteric viruses. Nat Rev Microbiol 14:197–204. https://doi.org/10.1038/nrmicro.2015.25

20 King KC, Brockhurst MA, Vasieva O, Paterson S, Betts A, Ford SA, Frost CL, Horsburgh MJ, Haldenby S, Hurst GD (2016) Rapid evolution of microbe-mediated protection against pathogens in a worm host. ISME J 10:1915–1924. https://doi.org/10.1038/ismej.2015.259

21 Kuss SK, Best GT, Etheredge CA, Pruijssers AJ, Frierson JM, Hooper LV, Dermody TS, Pfeiffer JK (2011) Intestinal microbiota promote enteric virus replication and systemic pathogenesis. Science 334:249–252. https://doi.org/10.1126/science.1211057

22 Kuyateh O, Obbard DJ (2023) Viruses in laboratory drosophila and their impact on host gene expression. Viruses 15:1849. https://doi.org/10.3390/v15091849

23. Lambrechts L, Saleh M-C (2019) Manipulating mosquito tolerance for arbovirus control. Cell Host Microbe 26:309–313. https://doi.org/10.1016/j.chom.2019.08.005

24. Lauring AS, Andino R (2010) Quasispecies theory and the behavior of RNA viruses. PLoS Pathog 6:e1001005. https://doi.org/10.1371/journal.ppat.1001005

25. Martins R, McCracken A, Simons M, Henriques C, Rera M (2018) How to catch a Smurf? – Ageing and beyond… in vivo assessment of intestinal permeability in multiple model organisms. Bio-protocol 8:3. https://doi.org/10.21769/BioProtoc.2722

26 Matos RC, Schwarzer M, Gervais H, Courtin P, Joncour P, Gillet B, Ma D, Bulteau AL, Martino ME, Hughes S, Chapot-Chartier M-P, Leulier F (2017) D-alanylation of teichoic acids contributes to *Lactobacillus plantarum*-mediated *Drosophila* growth during chronic undernutrition. Nat Microbiol 2(12):1635–1647. https://doi.org/10.1038/s41564-017-0038-x

27. McMullen JG, Bueno E, Blow F, Douglas AE (2021) Genome-inferred correspondence between phylogeny and metabolic traits in the wild Drosophila gut microbiome. Genome Biol Evol 13(8):evab127. https://doi.org/10.1093/gbe/evab127

28. Nigg JC, Mongelli V, Blanc H, Saleh MC (2021) Innovative toolbox for the quantification of Drosophila C virus, Drosophila A virus, and Nora virus. J Mol Biol 433:167308. https://doi.org/10.1016/j.jmb.2021.167308

29. Nigg JC, Castelló-Sanjuán M, Blanc H, Frangeul L, Mongelli V, Godron X, Bardin AJ, Saleh MC (2024) Viral infection disrupts intestinal homeostasis via Sting-dependent NF-κB signaling in drosophila. Curr Biol 34:2785–2800. https://doi.org/10.1016/j.cub.2024.05.009

30. Pfeiffer JK, Virgin HW (2016) Viral immunity: transkingdom control of viral infection and immunity in the mammalian intestine. Science 351:aad5872. https://doi.org/10.1126/science.aad5872

31 Putri GH, Anders S, Pyl PT et al (2022) Analysing high-throughput sequencing data in python with HTSeq 2.0. Bioinformatics 38:2943–2945. https://doi.org/10.1093/bioinformatics/btac166

32 Råberg L, Sim D, Read AF (2007) Disentangling genetic variation for resistance and tolerance to infectious diseases in animals. Science 318:812–814. https://doi.org/10.1126/science.1148526

33 Ren C, Webster P, Finkel SE, Tower J (2007) Increased internal and external bacterial load during Drosophila aging without lifespan trade-off. Cell Metab 6:144–152. https://doi.org/10.1016/j.cmet.2007.06.006

34 Rera M, Clark RI, Walker DW (2012) Intestinal barrier dysfunction links metabolic and inflammatory markers of aging to death in drosophila. Proc Natl Acad Sci U S A 109:21528–21533. https://doi.org/10.1073/pnas.1215849110

35 Robinson CM, Pfeiffer JK (2014) Viruses and the microbiota. Annu Rev Virol 1:55–69. https://doi.org/10.1146/annurev-virology-031413-085550

36 Romano V, Lussiana A, Monteith KM et al (2022) Host genetics and pathogen species modulate infection-induced changes in social aggregation behaviour. Biol Lett 18:20220233. https://doi.org/10.1098/rsbl.2022.0233
37 Ryu JH, Kim SH, Lee HY, Bai JY, Nam YD, Bae JW, Lee DG, Shin SC, Ha EM, Lee WJ (2008) Innate immune homeostasis by the homeobox gene caudal and commensal-gut mutualism in drosophila. Science 319:777–782. https://doi.org/10.1126/science.1149357
38 Segrist E, Miller S, Gold B, Li Y, Cherry S (2024) Tissue specific innate immune responses impact viral infection in drosophila. PLoS Pathog. https://doi.org/10.1371/journal.ppat.1012672
39 Shin SC, Kim SH, You H, Kim B, Ko AC, Kim SE, Kwon YM, Ryu JH, Lee WJ (2011) Drosophila microbiome modulates host developmental and metabolic homeostasis via insulin signaling. Science 334:670–674. https://doi.org/10.1126/science.1212782
40 Silva JMF, Nagata T, Melo FL, Elena SF (2021) Heterogeneity in the response of different subtypes of *Drosophila melanogaster* midgut cells to viral infections. Viruses 13:2284. https://doi.org/10.3390/v13112284
41 Simms EL, Triplett J (1994) Costs and benefits of plant responses to disease: resistance and tolerance. Evolution 48:1973–1985. https://doi.org/10.1111/j.1558-5646.1994.tb02227.x
42 Staubach F, Baines JF, Künzel S et al (2013) Host species and environmental effects on bacterial communities associated with drosophila in the laboratory and in the natural environment. PLoS One 8:e70749. https://doi.org/10.1371/journal.pone.0070749
43 Storelli G, Defaye A, Erkosar B, Hols P, Royet J, Leulier F (2011) *Lactobacillus plantarum* promotes Drosophila systemic growth by modulating hormonal signals through TOR-dependent nutrient sensing. Cell Metab 14:403–414. https://doi.org/10.1016/j.cmet.2011.07.012
44 Sun H, Longdon B, Raymond B (2025) Effect of the microbiome on pathogen susceptibility across four Drosophilidae species. bioRxiv. https://doi.org/10.1101/2025.10.22.683894
45 Vignuzzi M, Stone JK, Arnold JJ et al (2006) Quasispecies diversity determines pathogenesis through cooperative interactions in a viral population. Nature 439:344–348. https://doi.org/10.1038/nature04388
46 Webster CL, Waldron FM, Robertson S et al (2015) The discovery, distribution, and evolution of viruses associated with *Drosophila melanogaster*. PLoS Biol 13:e1002210. https://doi.org/10.1371/journal.pbio.1002210
47 Winans NJ, Walter A, Chouaia B et al (2017) A genomic investigation of ecological differentiation between free-living and Drosophila-associated bacteria. Mol Ecol 26:4536–4550. https://doi.org/10.1111/mec.14232
48. Wong CNA, Ng P, Douglas AE (2011) Low-diversity bacterial community in the gut of the fruitfly *Drosophila melanogaster*. Environ Microbiol 13(7):1889–1900. https://doi.org/10.1111/j.1462-2920.2011.02511.x
49. Wu P, Sun P, Nie K et al (2019) A gut commensal bacterium promotes mosquito permissiveness to arboviruses. Cell Host Microbe 25:101–112e5. https://doi.org/10.1016/j.chom.2018.11.004
50 Zheng J, Wittouck S, Salvetti E et al (2020) A taxonomic note on the genus *Lactobacillus*: description of 23 novel genera, emended description of the genus *Lactobacillus* Beijerinck 1901, and union of *Lactobacillaceae* and *Leuconostocaceae*. Int J Syst Evol Microbiol 70:2782–2858. https://doi.org/10.1099/ijsem.0.004107